Reverse-time migration for tilted TI media

Xiang Du, John C. Bancroft, and Larry R. Lines. CREWES, University of Calgary

Summary

Seismic anisotropy in dipping shales results in imaging and positioning problems for underlying structures. We develop a reverse-time anisotropic depth migration approach for P-wave and SV-wave seismic data in transversely isotropic (TI) media with a tilted axis of symmetry normal to bedding. Based on an accurate phase velocity formula, the wave equation of weak anisotropy for P-wave and SV-wave in tilted transversely isotropic (TTI) media is derived from a P and SV dispersion relationship. The accuracy of the P-wave equation and the SV-wave equation are analyzed and compared with other acoustic wave equations for TTI media. The pseudo-spectral method is used to solve these equations implementing reverse-time migration. The resulting anisotropic depth-migration algorithm is applied to numerical seismic data and physical-model seismic data. According to the comparison between the isotropic and anisotropic migration results, the reverse-time anisotropic depth migration offers significant improvements in positioning and reflector continuity over those obtained using isotropic algorithms.

Introduction

Much hydrocarbon resource exploration and development involves classic dipping anisotropic sequences, and thick anisotropic sequences of dipping sandstones and shales often overlie the reservoir in fold and thrust belts, such as in the Canadian Foothills (Isaac and Lawton, 1999). In these cases, during data processing - particularly depth migration, with the isotropic migration algorithm or VTI assumption – there will be imaging problems and mispositioning errors. Anisotropic depth migration is required to correctly locate images when TTI strata are present. Alkhalifah (1994) proposed Gaussian beam depth migration for VTI media. Vestrum et al. (1999) adopted a ray-tracing algorithm to image structures below dipping TI media. Ferguson and Margrave (2000) addressed nonstationary phase-shift for TI media. In this paper, we present a reverse-time migration for tilted transverse isotropic media. We derive the P-wave equation and SV-wave equation for TTI media from Tsvankin's (1996) phase velocity formula. We also analyze the accuracy of these equations. Examples of impulse response and physical models are shown to demonstrate the excellent ability of reverse-time migration in dipping angle.

Principle

To simulate P-wave propagation in a vertical axis of symmetry (VTI) medium, Alkhalifah (2000) proposed an acoustic wave equation by simply setting the shear wave velocity to zero. He showed that the new acoustic VTI wave equation yields a kinematically good approximation of P-wave propagation as compared to the full elastic solution in VTI media. Zhang et al. (2003) extended the acoustic wave equation for VTI media to one for TTI media. In fact, contrary to the conventional wisdom that setting Vs_0 equal to 0 eliminates shear waves, the acoustic wave equation introduces diamond-shape artifacts, which means that it doesn't eliminate the shear wave phase velocity in other directions. Grechka et al. (2004) discussed the shear waves in acoustic anisotropic media. Although Alkhalifah proposed to place a big enough isotropic layer between the source and the first anisotropic medium, this imposes limitations to his formulation not only for modeling anisotropic cases, but for possible extensions to other seismic processing stages. In fact, weak anisotropy is a useful assumption in many real systems (Thomsen, 1986). We start with the VTI phase-velocity equation (Tsvankin, 1996) written as

$$\frac{V^2(\theta,\phi)}{V_{p0}^2} = 1+\varepsilon\sin^2(\theta-\phi)-\frac{f}{2} \pm \frac{f}{2}\sqrt{(1+\frac{2\varepsilon\sin^2(\theta-\phi)}{f})^2-\frac{2(\varepsilon-\delta)\sin^2 2(\theta-\phi)}{f}}$$

and make a quadratic approximation for weakly anisotropic media. By rotating the symmetry axis from vertical to a titled angle ϕ, we can get the phase velocity for P and SV waves in the direction measured from the vertical direction. The P and SV wave equation in wave-number and time domain are shown as follows:

$$\begin{aligned}\frac{\partial^2 U(k_x,k_z,t)}{\partial t^2} = V_{p0}^2[&k_x^2+k_z^2+(2\delta\sin^2\phi\cos^2\phi+2\varepsilon\cos^4\phi)\frac{k_x^4}{k_x^2+k_z^2}\\ &+(2\delta\sin^2\phi\cos^2\phi+2\varepsilon\sin^4\phi)\frac{k_x^4}{k_x^2+k_z^2}\\ &+(-\delta\sin^2 2\phi+3\varepsilon\sin^2 2\phi+2\delta\cos^2\phi)\frac{k_x^2k_z^2}{k_x^2+k_z^2}\\ &+(\delta\sin 4\phi-4\varepsilon\sin 2\phi\cos^2\phi)\frac{k_x^3k_z}{k_x^2+k_z^2}\\ &+(-\delta\sin 4\phi-4\varepsilon\sin 2\phi\sin^2\phi)\frac{k_z^3k_x}{k_x^2+k_z^2})]U(k_x,k_z,t)\end{aligned}$$

$$\begin{aligned}\frac{\partial^2 U(k_x,k_z,t)}{\partial t^2} = V_{s0}^2[&k_x^2+k_z^2+\frac{\sigma}{2}(2\sin^2 2\phi\frac{k_x^4+k_z^4-2k_x^2k_z^2}{k_x^2+k_z^2}+4\cos^2\phi)\frac{k_x^2k_z^2}{k_x^2+k_z^2}\\ &+4\varepsilon\sin 2\phi\cos^2\phi)\frac{k_xk_z(k_x^2-k_z^2)}{k_x^2+k_z^2}]U(k_x,k_z,t)\end{aligned}$$

$$\sigma = (\frac{V_{p0}}{V_{s0}})^2(\varepsilon-\delta)$$

To analyze the accuracy of the wave equations, the relationship between phase velocity and phase angle is discussed. We compare the difference among the weak

anisotropy formula, the Alkhalifah approximation formula and the exact P-wave phase velocity formula for TTI media. Figure 1 shows the phase velocity and phase angle curve with 0, 30, 60, and 90 degree dipping angle and epsilon=0.25, delta=0.1 for P-waves. There is hardly a difference among them for weak anisotropy media. Figure 2 corresponds to the SV case comparison between weak anisotropy and accurate the SV-wave phase velocity formula for the TTI media. There is some difference in the long offset position, but the near offset relationship is close enough to be used for migration and NMO analysis. In fact, with the third-order approximation from the exact SV phase velocity formula, the accuracy will be greatly improved, which also means increasing the computation time. Therefore the wave equations derived as above can be accurately used for tilted transversely isotropic media. Considering that the space and time are coupled, the wave equations are solved by the pseudospectral method. Since reverse-time migration shows excellent ability in full dipping angle imaging, the reverse-time scheme is used to implement migration for TTI media.

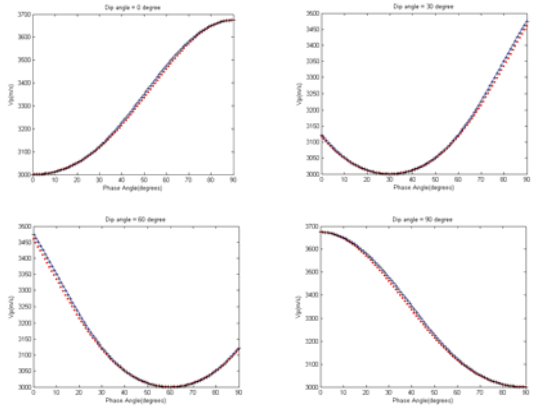

Figure 1. P-wave phase velocity. The black cross line corresponds to the Alkhalifah formula, the red one to the weak anisotropy formula, and the solid one to the exact formula.

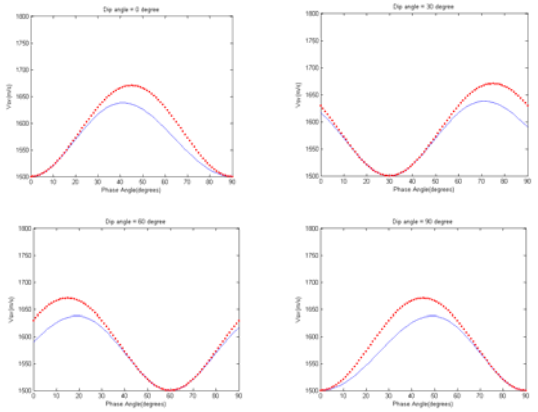

Figure 2. SV-wave phase velocity. The red dots correspond to the weak anisotropy formula and the solid one to the exact formula.

Numerical and physical examples

To verify reverse-time migration's effectiveness and accuracy, three examples are chosen, including P-wave and SV-wave impulse responses and two physical experiments. P- and SV-wave impulse responses show excellent dipping angle imaging ability. Two physical experiments, an isotropic reef with a TTI overburden and a TTI thrust sheet in an isotropic background, exhibit the accurate image positioning of reverse-time anisotropic migration while reverse-time isotropic migration gives considerable errors in physical position and energy focus.

P and SV wave impulse response

Figure 3 shows the P-wave impulse response in a tilted TI medium with tilt angles of 0, 30, 60, and 90 degrees. Figure 4 corresponds to the SV-wave impulse response. The velocity of the P-wave is 3500m/s and that of the SV-wave is 1500m/s. The homogenous medium has Thomsen anisotropy parameters delta=0.1 and epsilon=0.25. As mentioned above, the migration results have clear energy in dipping angle up to 90 degrees. As tilt angles change, the symmetric axis keeps pace with them. At the same time, considering the anisotropy effect, the waterfronts of P-waves and SV-waves are totally different from the circular ones of an isotropic medium.

Depth migration for isotropic reef with a TTI overburden

Seismic data from an anisotropic physical model described by Isaac and Lawton (1999) were used to test the migration algorithm. The cross-section of this model is shown in Figure 5; it includes a TI overburden layer, 1500 m thick, with the axis of symmetry dipping at 45^0. The layer has parameters V_0=2945m/s, $\varepsilon = 0.241$, and $\delta = 0.100$. An isotropic layer that contains a reef with V_0=2740m/s underlies this anisotropic overburden. Figure 6 shows a zero-offset seismic section with the surface wave muted. Migration of the zero-offset section by isotropic reverse-time migration yields an image of the reef edge which is displaced by about 350m to the left of its true position (Figure 7). Migration by TTI reverse-time migration correctly positions the edge of reef, as shown in Figure 8. In this case, the input to the migration consisted of a grid containing values of v_0 , ε , δ , and tilt of the symmetry axis at each node. Although there are some artifacts caused by interface reflections, they don't affect the basement. The reef is imaged to its true position.

Migration for TTI thrust sheet in an isotropic background

The second physical model is that of a flat reflector overlain by a TI thrust sheet embedded in an isotropic background. The thrust sheet is composed of four blocks (Figure 9); each with a unique axis of symmetry. They have parameters of V_0=2925m/s, $\varepsilon = 0.224$, and $\delta = 0.100$. The

isotropic background has a flat basement with Vp=2740m/s. The zero-offset seismic section is given in Figure 10. Similar to the first physical model, we adopt the isotropic reverse-time migration and anisotropy reverse-time migration for seismic section. With the velocity Vp=2925m/s for the thrust sheet, the isotropic reverse-time migration result (Figure 11) produces a partial flat basement, whereas the basement beneath thrust sheets exhibits substantial pull up and the energy cannot be focused. The interface between first block and second block is incorrectly positioned. Migration by anisotropic reverse-time migration (Figure 12) does a better job of positioning the reflectors and has nearly flattened the basement reflection though the energy isn't consistent. The crossing energy at the base reflector between 2000 and 3300m is believed to indicate a shadow zone caused by the high-velocity thrust sheet overlying slower material. The shadow zone is a result of the zero-offset geometry of the recording. In fact, migration of the prestack data by source-gather migration will fill in the shadow zone due to the multiplicity of ray paths afforded by the prestack geometry.

Conclusion and future work

The wave equation of weak anisotropy for P-waves and SV-waves in tilted transversely isotropic (TTI) media is derived. The accuracy of the P-wave equation and the SV-wave equation is analyzed and compared with other acoustic wave equations for TTI media. The pseudo-spectral method is used to solve these equations implementing reverse-time migration. According to the migration result of physical-model seismic data, anisotropic reverse-time migration shows excellent accuracy for TTI media. The method is encouraging and promising. In the future, an anisotropic prestack reverse-time migration algorithm will be implemented and used to migrate the field seismic data. In addition, using the SV wave equation, an algorithm for prestack and poststack converted wave data will be developed.

Acknowledgements

We should express our thanks to Dr. Helen Isaac and Dr. Chuck Ursenbach who prepared the model data for us and gave a lot of help. Xiang Du also thanks CREWES for financial support and the SEG and CSEG for scholarships.

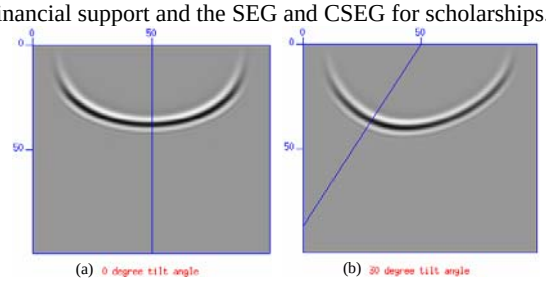

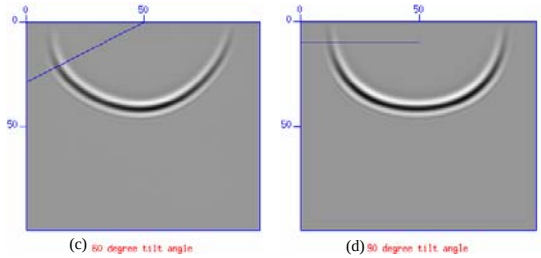

Figure 3. P- wave impulse response. (a), (b),(c) and (d) correspond to the result of a tilt angle of 0, 30, 60, and 90 degrees.

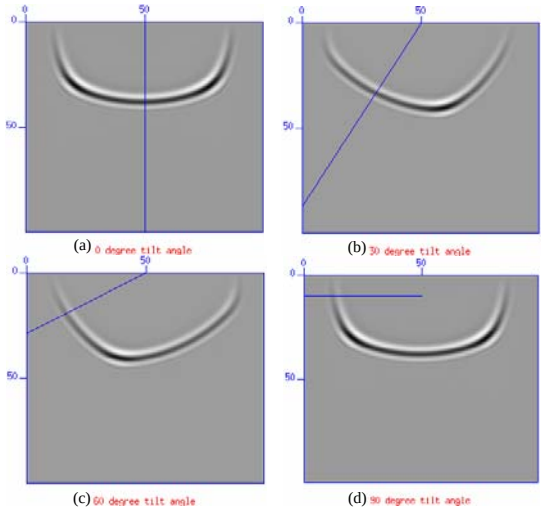

Figure 4. SV-wave impulse response. (a), (b),(c) and (d) correspond to the result of a tilt angle of 0, 30, 60, and 90 degrees.

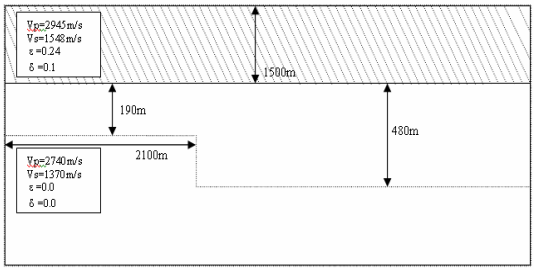

Figure 5. Isotropic reef with a TTI overburden.

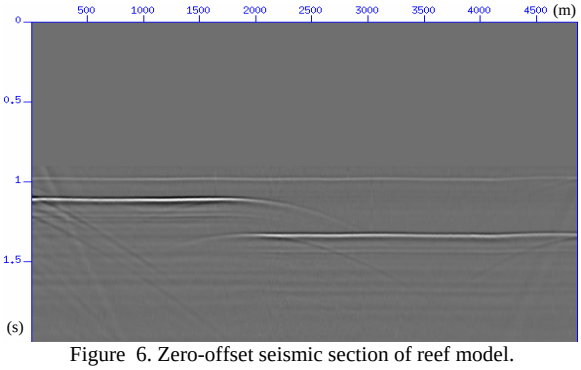

Figure 6. Zero-offset seismic section of reef model.

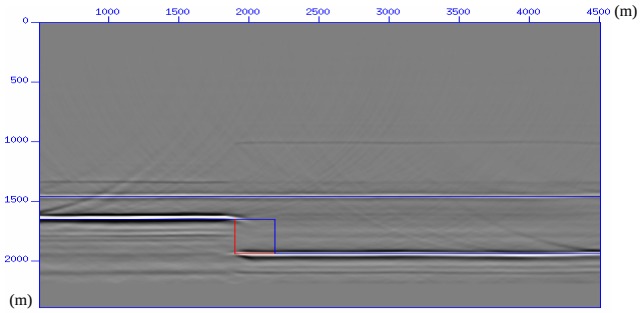

Figure 7. Isotropic migration result of reef model

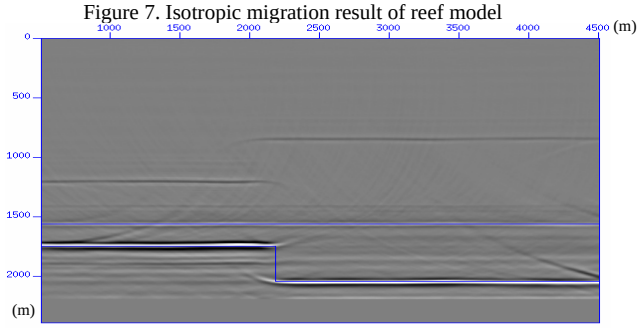

Figure 8. Anisotropic migration result of reef model

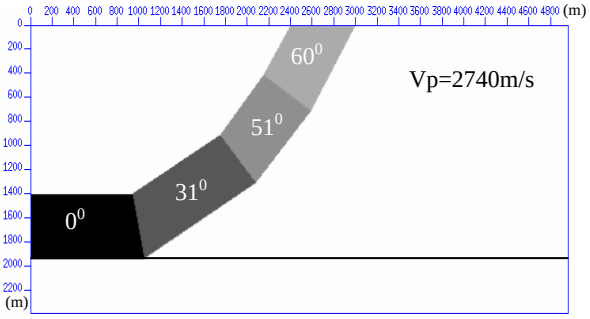

Figure 9. TTI thrust model.

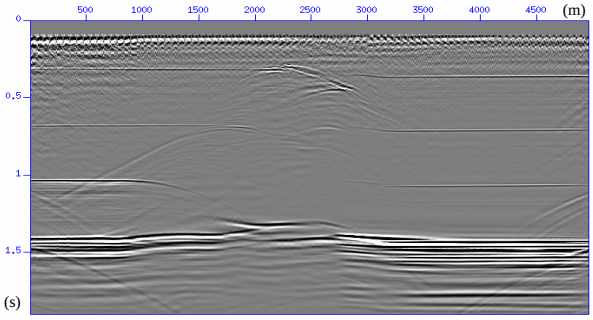

Figure 10. Zero-offset seismic section of TTI thrust model.

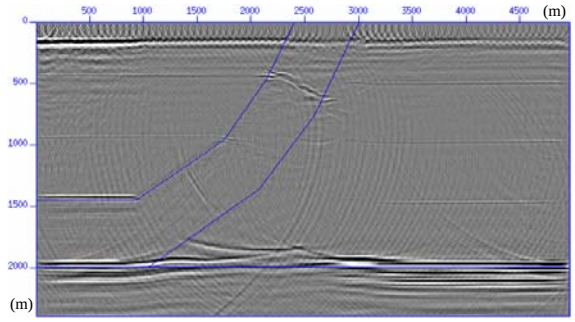

Figure 11. Isotropic migration result of TTI thrust model.

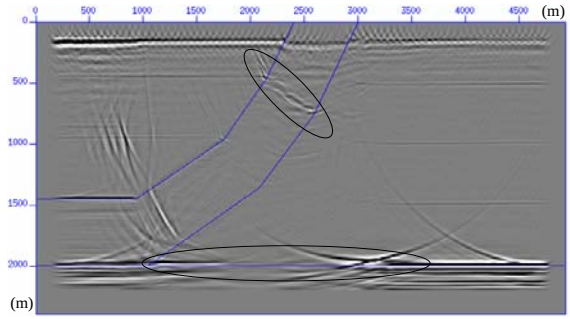

Figure 12. Anisotropic migration result of TTI thrust model.

References

Alkhalifah, T., 1995, Gaussian beam depth migration for anisotropic media: Geophysics, 60, 1474-1484.

Alkhalifah, T., 2000, An acoustic wave equation for anisotropic media: Geophysics, 65, 1239-1250.

Ferguson, R. and Margrave G. F., 1999, Prestack depth migration in anisotropic media by nonstationary phase shift: CREWES Research Report 1999 (available at www.crewes.org).

Grechka, V., Zhang, L. and Rector, J., 2004, Shear waves in acoustic anisotropic media: Geophysics, 69, 576-582.

Isaac, J. H., and Lawton, D. C., 1999, Image mispositioning due to dipping TI media: A physical seismic study: Geophysics, 64, 1230-1238.

Vestrum, R. W., Lawton, D. C. and Schmid, R., 1999, Imaging structures below dipping TI media: Geophysics, 64, 1239-1246.

Thomsen, L., 1986, Weak elastic anisotropy: Geophysics, 51, 1954–1966.

Tsvankin, I., 1996, P-wave signatures and notation for transversely isotropic media: An overview: Geophysics, 61, 467-483.

Zhang, L., Rector, J. W., and Hoversten, G. M., 2003, An acoustic wave equation for modeling in tilted TI media: 73rd Annual International Meeting, SEG, Expanded Abstracts, 153–156.